

# Effects of Parallel Contact Cooling on Pulsed-Type, Bipolar Radiofrequency-Induced Tissue Reactions in an in vivo Porcine Model

Sung Bin Cho<sup>1,\*</sup>, Yea-Jin Lee<sup>2,\*</sup>, Sun Young Kang<sup>3</sup>, Min Choi<sup>3</sup>, Bora Kim<sup>3</sup>, Jin-Chul Ahn<sup>2</sup>

<sup>1</sup>Yonsei Seran Dermatology and Laser Clinic, Seoul, Korea; <sup>2</sup>Medical Laser Research Center, College of Medicine, Dankook University, Cheonan, Korea; <sup>3</sup>R&D Center, Shenb Co., Ltd, Seoul, Korea

\*These authors contributed equally to this work

Correspondence: Jin-Chul Ahn, Medical Laser Research Center, College of Medicine, Dankook University, Cheonan, 31116, Korea, Tel +82.41-550-1811, Fax +82.41-550-7706, Email jcahn@dankook.ac.kr

**Background:** Skin cooling during laser or radiofrequency (RF) treatments is a method to minimize thermal damage to the epidermis, reduce pain, and decrease post-treatment downtime. We evaluated the effect of parallel contact cooling (PCC) on RF-induced thermal reactions in minipig skin in vivo after bipolar microneedling RF treatment.

**Methods:** RF treatments were administered at frequencies of 0.5, 1, and 2 MHz with single (500 ms), six (1000 ms), and ten (5000 ms) sub-pulse packs to minipig skin with or without PCC. Subsequently, thermometric imaging and histology were used to analyze skin reactions to RF.

**Results:** Thermometric images showed that PCC promptly lowered skin temperature in the RF-treated area, with this effect persisting for over 60s. Regardless of the PCC, RF treatments lasting for 500 ms with a single pulse pack resulted in peri-electrode coagulative necrosis (PECN) zones and inter-electrode non-necrotic thermal reaction (IENT) zones in the dermis. In contrast, treatment lasting 5000 ms with 10 sub-pulse packs produced distinct IENT without notable PECN over a wide dermal area. Skin specimens obtained at 1 h and 3, 7, and 14 days after PCC-assisted RF treatments showed a higher degree of thermal tissue reactions in the deeper dermal regions compared to those after RF treatments without PCC.

**Conclusion:** PCC-assisted RF treatment, utilizing an invasive bipolar microneedling device, enhanced RF-induced skin reactions in the mid to deep dermis while preserving the epidermis and upper papillary dermis from excessive thermal tissue injury.

**Keywords:** radiofrequency, parallel contact cooling, thermoelectric cooling, bipolar, alternating current, gated pulse, tissue reaction, porcine model

## Introduction

Bipolar, alternating current, microneedling radiofrequency (RF) devices have been used in the treatment of various dermatological disorders.<sup>1-4</sup> RF treatments, administered through insulated or non-insulated microneedle electrodes, can take the form of a single pulse pack or multiple sub-pulse packs.<sup>5-7</sup> RF treatment generates different patterns of thermal tissue reactions, influenced by several parameters, including RF frequency, power, conduction time, number of sub-pulse packs, on-time of each sub-pulse pack, off-time between sub-pulse packs, and the type of microneedles used.<sup>5-7</sup> RF treatment is known to induce various tissue reactions, including non-necrotic thermal reactions with reversible cell damage at temperatures of 40–45 °C, coagulation necrosis at temperatures exceeding 60 °C, and tissue desiccation above 100 °C.<sup>1,8</sup> However, the specific treatment parameters that induce RF-induced thermal reactions have not been fully elucidated.

In a recent in vivo study on rat skin, we described the thermal tissue reactions resulting from 1-MHz RF treatments with insulated microneedle electrodes. Specifically, we focused on peri-electrode and inter-electrode areas in the dermis

under varying conduction times and numbers of sub-pulse packs.<sup>5</sup> We observed that increasing the total RF conduction time from 200 to 800 ms under a single pulse pack setting led to an expansion of peri-electrode coagulation necrosis (PECN), which was histologically presented as a relatively well-demarcated round to oval-shaped zone of tissue coagulation along the penetrating electrode.<sup>5</sup> The location and degree of coagulation necrosis were influenced by skin tissue impedance and adjacent adnexal structures. Conversely, under multiple sub-pulse pack settings, increasing the number of sub-pulse packs reduced or eliminated the PECN zone.<sup>5</sup> Interestingly, with extended off-time settings between sub-pulse packs, we observed a more distinct inter-electrode non-necrotic thermal reaction (IENT) zone in the upper papillary, mid, deep dermis, and subcutaneous fat layers. Therein, IENT was histologically presented as a relatively ill-demarcated zone of eosinophilic cellular and stromal changes between the penetrating electrodes without remarkable tissue necrosis. This effect was more prominent when using seven or ten sub-pulse packs, despite a significantly shorter RF conduction time and longer off-time.<sup>5</sup>

To minimize thermal damage in the epidermis, alleviate pain, and reduce post-treatment erythema, skin cooling methods have been adapted into energy-delivering treatments.<sup>9,10</sup> These methods of skin cooling can be categorized into contact/noncontact cooling and pre-cooling/parallel cooling/post-cooling.<sup>10</sup> In the current study, we aimed to histologically evaluate the effect of parallel contract cooling (PCC) on RF-induced thermal tissue reactions in minipig skin after bipolar, alternating current, and microneedling RF treatment. We administered RF treatments at frequencies of 0.5, 1, and 2 MHz, with varying total treatment time settings, including 500 ms for a single pulse pack, 1000 ms for six sub-pulse packs, and 5000 ms for ten sub-pulse packs. These RF treatments were delivered to minipig skin in vivo with or without PCC. During the RF treatment, we monitored the porcine skin's surface temperature using real-time noncontact infrared thermometry. Subsequently, we collected minipig skin specimens at different time points (1 h and 3, 7, and 14 days) post-RF treatment for microscopic analysis.

## Materials and Methods

### Bipolar RF Device with PCC

A bipolar alternating current RF device (VIRTUE RF™; Shenb Co., Ltd., Seoul, Korea) was used to analyze RF-induced tissue reactions in in vivo porcine model as described in the previous reports.<sup>5,6</sup> The device delivered RF energy at the frequencies of 0.5, 1, and 2 MHz through 36 insulated microneedle electrodes at the diameter of  $300 \pm 5 \mu\text{m}$  in a  $15 \times 15\text{-mm}$  disposable tip (Deep RF™ 36 tip; Shenb Co., Ltd.). The penetrating electrodes were regularly arranged in a  $6 \times 6$  pattern with the microneedles spaced 3 mm apart. The length of a non-insulated electrode tip was  $300 \mu\text{m}$ . In this study, a PCC with a cooled sapphire metal plate and thermoelectric elements was integrated into a handpiece. The temperature of the chilled plate was regulated at  $15 \pm 0.5 \text{ }^\circ\text{C}$  for this experiment.

### Treatment of Minipig Skin with PCC-Assisted Bipolar RF

Four 10-week-old female minipigs (*Sus scrofa domestica*) were purchased (M-pig®; CRONEX Inc., Cheongju, Korea), and the experiments were performed when the minipigs were at the age of 12 weeks and weighed 55–75 kg. General anesthesia was administered via an intramuscular injection of 5-mg/kg tiletamine/zolazepam and 2-mg/kg xylazine. Subsequently, endotracheal intubation was performed, and the pig was ventilated with oxygen and 2% isoflurane. Intravenous hydration through the superficial auricular vein with 0.9% normal saline at 25 mL/hour was maintained during the experiments. After gentle removal of hair on the abdomen, the lesions were cleaned with soap and 70% alcohol. The skin was marked with black ink to outline the grids for each treatment setting (1.5 cm diameter/grid; 40 grids/minipig; a total of 160 grids).

Then, RF treatment at the frequencies of 0.5, 1, and 2 MHz was performed on each grid of the experimental rat at a power of 35 W and an electrode penetration depth of 1.5 mm over one pass. For all treatments, the total RF conduction time was 500 ms. The total treatment time was designated as the sum of the RF conduction time and off-time, and was experimentally regulated to be 500, 1000, and 5000 ms for single, six, and ten pulse packs with 0, 500, and 4500 ms of off-time, respectively. The RF treatments were delivered to minipigs with or without PCC (Figure 1). No pretreatment topical anesthesia or pre- or post-cooling was applied and no prophylactic topical or systemic antibiotics or steroids were

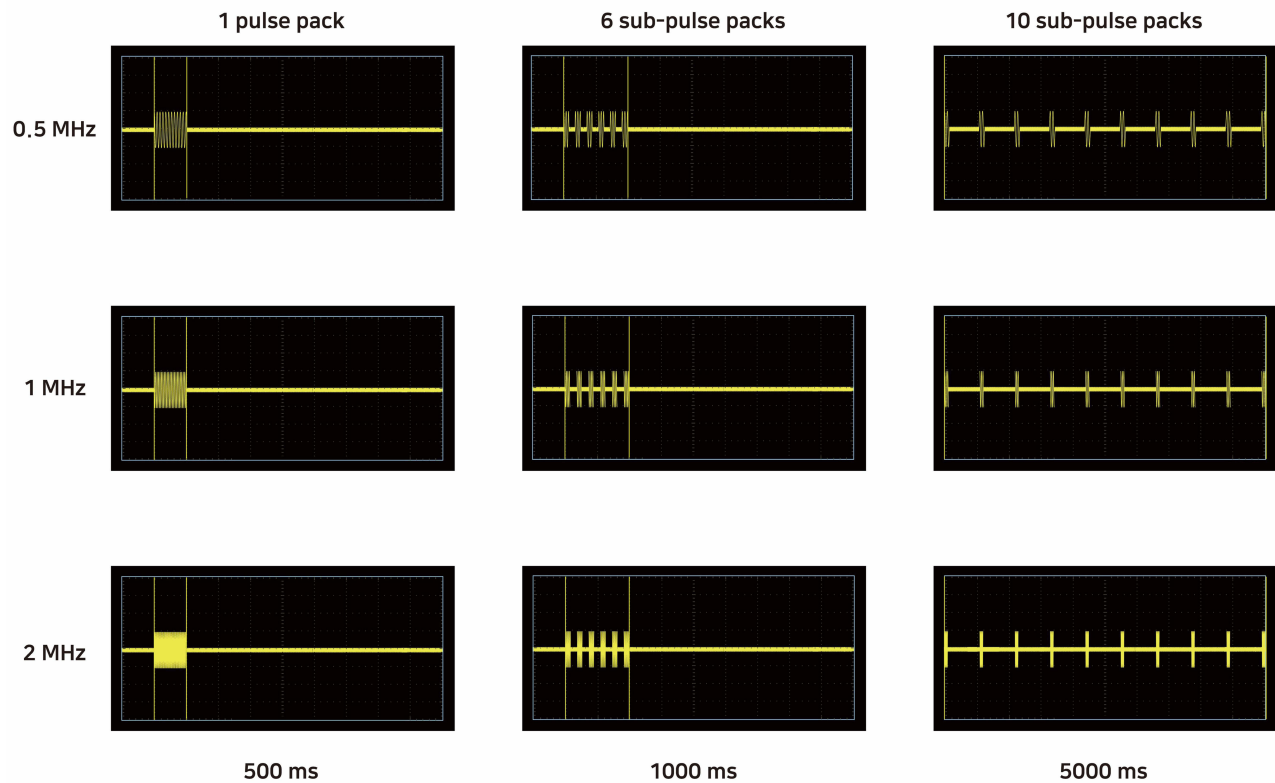


**Figure 1** Schematic illustrations of experimental parameters for 0.5-, 1-, and 2-MHz, invasive bipolar radiofrequency (RF) treatment with or without parallel contact cooling (PCC) on in vivo minipig tissue.

administered after RF treatment. Ethical approval was obtained from the Ethics Committee of the Institutional Animal Care and Use Committee of CRONEX Inc. (Cheongju, Korea; CRONEX-IACUC:202210005). All in vivo experiments using minipigs were performed in accordance with the Institutional Animal Care and Use Committee and the National Institute of Health Guidelines for the Care and Use of Laboratory Animals.

## Thermometric and Histological Evaluation

Noncontact infrared thermometric measurements of RF-treated minipig skin were performed using a thermal imaging camera at 10,800 pixels (FLIR E5; FLIR Systems Inc., Wilsonville, OR, USA). Thermal values were measured using the thermal images, which were obtained at baseline; immediately after; and 10, 20, 30, 40, 50, and 60s after RF treatment while keeping a 15-cm distance between the surface of the porcine skin and the camera.

Each experimental minipig was euthanized according to standard protocols to humanely obtain the tissue samples. Full-thickness tissue specimens, which contained the epidermis, dermis, and subcutaneous fat, were sampled one hour and 3, 7, and 14 d after treatment, fixed in 10% buffered formalin, and embedded in paraffin. Four- $\mu$ m thickness, 15 to 30 serial tissue sections of each experimental setting were stained with hematoxylin and eosin for microscopic evaluation.

## Results

### Thermometric Change in Minipig's Skin After RF Treatment with PCC

Thermometric images obtained from a thermal imaging camera revealed elevations in tissue temperature at the RF-treated areas under all experimental settings. After adjusting the thermometric values of the baseline tissue temperature to 36 °C, the average surface temperatures of RF-treated in vivo minipig skin with and without PCC in each experimental setting were evaluated (Table 1). Compared to the baseline, RF treatment without PCC immediately resulted in a homogenous, well-demarcated, square-shaped zone of higher temperature, which macroscopically correlated with the

**Table I** Thermometric Values Measuring Surface Temperature of in vivo Minipig Skin After Invasive Bipolar Radiofrequency Microneedling Treatment with or Without Parallel Contact Cooling

Parallel Contact Cooling	Frequency (MHz)	Total Treatment Time (ms)	Sub-Pulse Packs (N)	Thermometric value* (°C)								
				Baseline	Immediate	10s	20s	30s	40s	50s	60s	
Off	0.5	500	1	36±0.7	38.6±0.6	39.1±0.3	39.2±0.4	39.3±0.2	39.7±0.2	39.6±1.3	39.7±0.5	
		1000	6	36±0.1	36.8±0.5	38.3±0.1	38.4±0.1	38.7±0.1	38.7±0.2	38.9±1	39.1±0.4	
		5000	10	36±0.2	37.1±0.1	37.8±0.3	38±0.1	38±0.2	37.70±0.3	37.7±0.6	37.7±0.5	
	1	500	1	36±0.1	38.6±0.2	38.7±0.1	39.3±0.1	39.4±0.1	39.4±0.2	40±1.3	40.2±0.1	
		1000	6	36±0.1	37.8±0.5	37.8±0.4	38±0.1	38.2±0.1	38.20±0.1	38.3±0.7	38.2±0.2	
		5000	10	36±0.1	37±0.2	37.4±0.2	37.5±0.1	37.6±0.3	37.6±0.3	37.6±0.3	37.6±0.1	
	2	500	1	36±0.1	37.2±0.2	38.3±0.1	38.9±0.2	39.1±0.4	39.1±0.2	39.2±1.1	39.4±0.5	
		1000	6	36±0.2	37.5±0.4	37.9±0.2	38±0.3	38.1±0.2	38.2±0.4	38.2±0.5	38.2±0.7	
		5000	10	36±0.1	36.4±0.1	36.6±0.1	37.4±0.1	37.5±0.1	37.6±0.1	37.6±0.3	37.7±0.2	
	On	0.5	500	1	36±0.6	28.4±1.5	33.8±1.1	34.2±0.9	34.6±0.8	34.9±0.5	34.9±0.5	34.8±0.5
			1000	6	36±1.5	29.4±1.6	34±0.7	34.6±0.7	34.8±0.6	34.8±0.4	35±0.5	35.3±0.4
			5000	10	36±1.1	26.8±1.8	33.3±1.3	33.7±1	34±0.8	34.1±0.8	34.1±0.7	34.5±0.6
1		500	1	36±1.2	28.6±1.3	34.3±0.9	34.9±0.5	35.2±0.5	35.1±0.4	35.4±0.4	35±0.5	
		1000	6	36±0.6	28.6±1.6	33.8±0.8	34.2±0.6	34.6±0.4	34.8±0.4	34.8±0.3	34.9±0.3	
		5000	10	36±1.3	28.2±0.4	34±0.4	34.5±0.8	34.8±0.6	34.8±0.7	34.9±0.4	35.1±0.3	
2		500	1	36±2.6	30.9±1.4	35.4±1.3	36±1.2	36.8±0.6	36.9±0.5	37±0.6	37±0.7	
		1000	6	36±2.5	29.9±0.9	34.5±0.7	35.4±0.5	35.9±0.5	36.2±0.4	36.1±0.3	36.4±0.3	
		5000	10	36±1.8	29.2±1.5	33.2±1.4	34.1±1	34.4±0.7	34.9±0.6	35.1±0.5	36.1±0.5	

Notes: \*Thermometric values of baseline tissue temperature were adjusted to 36°C. Values were presented as average ± standard deviation.

contact surface areas of the disposable tips (Figures 2A and B). The margin of the uncooled metal plate had a mildly lower temperature than the central RF-treated area. Nonetheless, thermal reactions in the RF-treated central areas were found to spread beyond the margin of the squared tip areas during the post-treatment 60-s timespan.

Immediately after treatment, the surface temperature of the RF-treated areas was notably lower under the RF treatment settings with PCC than at baseline (Figures 2C and D). Subsequently, the surface temperature of the RF-treated areas increased for 60s post-treatment. The margin of the cooled metal plate had a remarkably lower temperature compared to the central or surrounding areas. Interestingly, the thermometric images indicated that the low-temperature margin and high-temperature center areas merged over a duration of 60s. Moreover, the thermal reactions in the RF-treated central areas did not spread beyond the margin of the square-tip areas until 60s post-treatment.

## Radiofrequency Treatment-Induced Tissue Reactions Without PCC

The minipig skin specimens, which were obtained 1 h after RF treatment under various experimental conditions without PCC, generally exhibited two distinctive patterns of thermal tissue reactions in the dermis: 1) PECN zones, which were generated in the area of high tissue impedance or around hair follicles, and 2) IENT zones. At the frequency of 0.5 MHz and total RF conduction time of 500 ms, a marked PECN zone was found in the upper to mid-dermis and an IENT region in the mid-dermis without notable thermal injury in the epidermis (Figure 3A). Meanwhile, compared with the RF treatment of 500-ms duration, RF treatment at 0.5 MHz over 1000 ms presented notable but smaller PECN areas and wider and deeper IENT areas in the dermis (Figure 3B). Additionally, an IENT area was found in the mid-to-deep dermis with the experimental condition of 0.5 MHz over 5000 ms but no remarkable PECN area was found (Figure 3C).

RF-induced upper dermal PECN and mid-to-deep dermal IENT areas were observed at a frequency of 1 MHz over 500 ms (Figure 3D). RF treatment at 1 MHz over 1000 ms exhibited notable PECN and IENT in the dermis, and the patterns were found to be more widely and deeply distributed, but the degree of thermal tissue reactions was lower than that at the 500-ms treatment (Figure 3E). Further, RF treatment at 1 MHz over 5000 ms generated IENT in the dermis but no remarkable PECN (Figure 3F). Therefore, the area of the IENT was wider and deeper in the dermis, but the degree of thermal tissue reaction was remarkably lower than that in the 1-MHz experiments delivered over 500- and 1000-ms experiments.

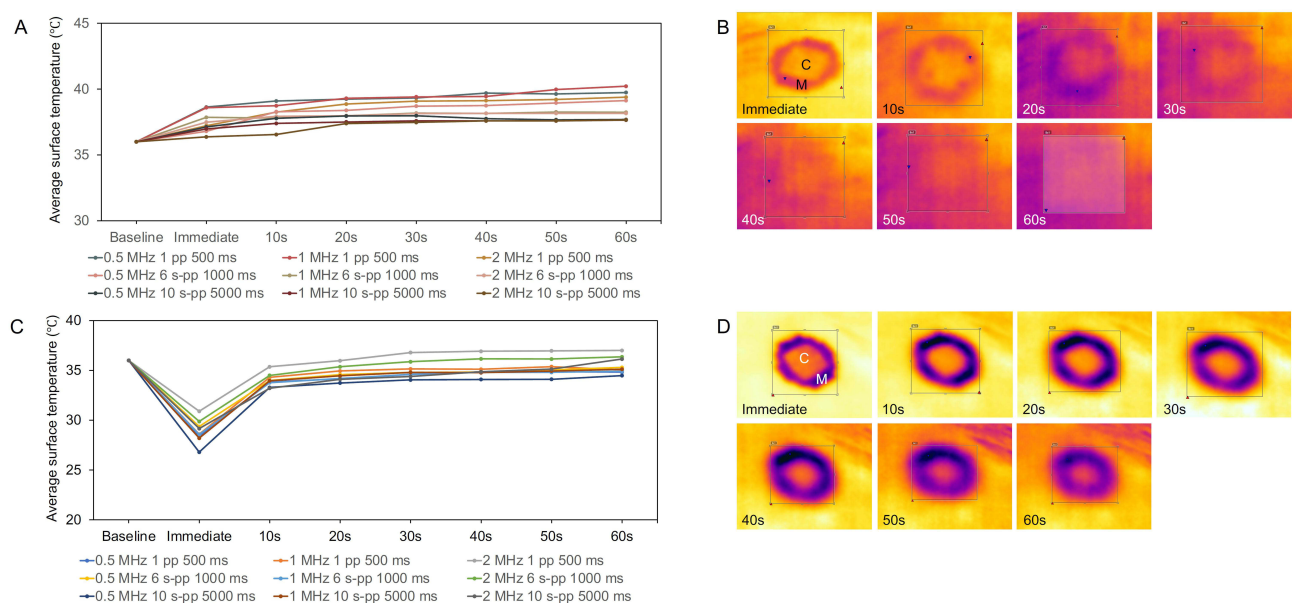


**Figure 2** Thermometric values measuring surface temperature of in vivo minipig skin after invasive bipolar RF treatment with or without PCC. (A) Thermometric values and (B) images after RF treatment without PCC, measured from baseline to 60s. (C) Thermometric values and (D) images after PCC-assisted RF treatment. Thermometric values of baseline tissue temperature were adjusted to 36 °C. pp, pulse pack. s-pp, sub-pulse packs. C, center of metal plate, which corresponded with the area of RF treatment; M, margin of metal plate.

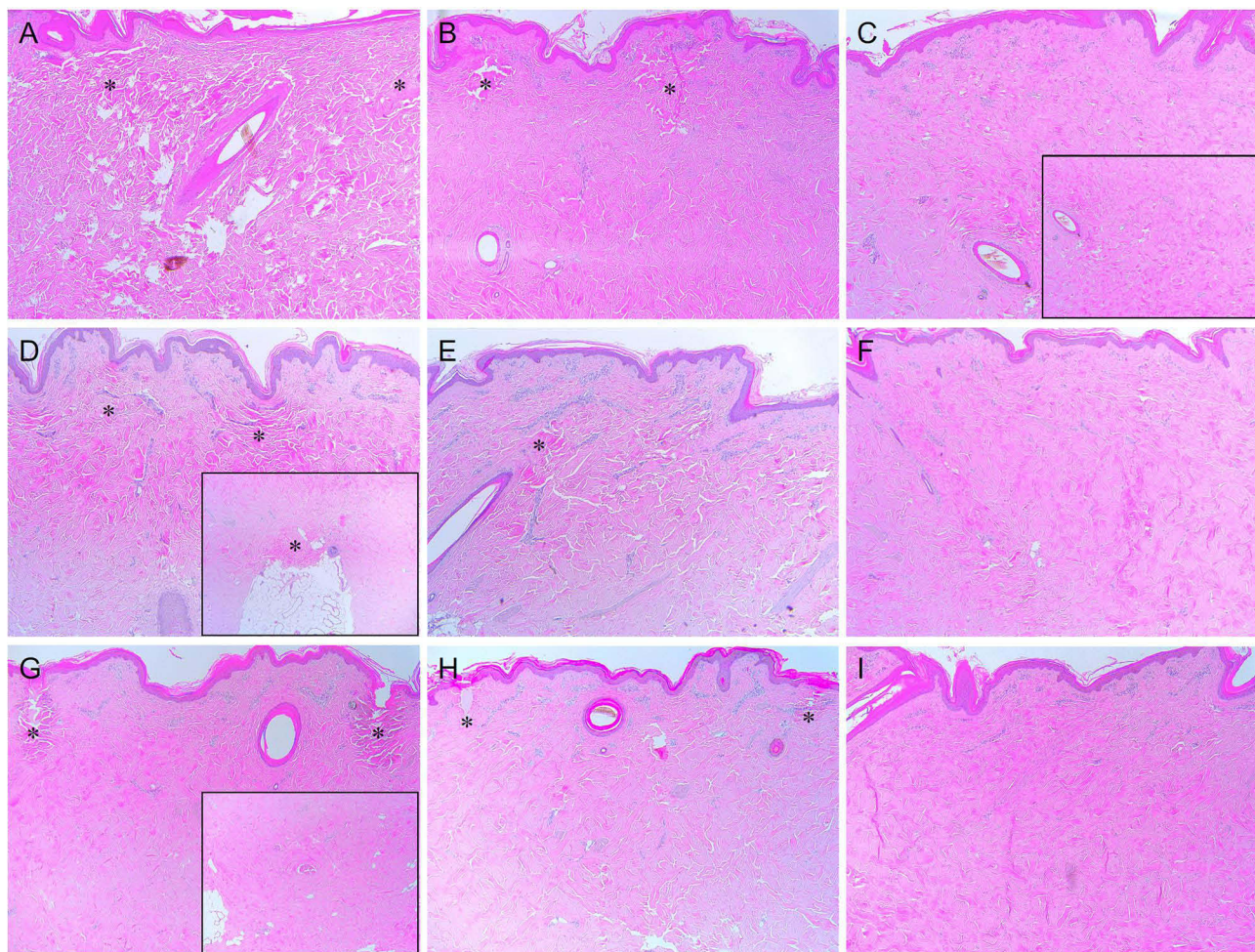


**Figure 3** Immediate tissue reactions in in vivo minipig skin after RF treatment without PCC. The skin of minipig was treated with RF at the frequencies of (A-C) 0.5 MHz, (D-F) 1 MHz, and (G-I) 2 MHz and the total treatment time and number of sub-pulse packs of (A, D, G) 500 ms and single pulse pack, (B, E, H) 1000 ms and six sub-pulse packs, and (C, F, I) 5000 ms and 10 sub-pulse packs. Inlet, histological photographs showing the mid and deep dermis. Asterisks, peri-electrode coagulative necrosis zones. Hematoxylin and eosin staining. Original magnification  $\times 40$ .

RF-induced upper dermal PECN and mid-to-deep dermal IENT were observed at a frequency of 2 MHz over 500 ms (Figure 3G). The 1000-ms, 2-MHz RF treatment exhibited remarkable IENT in the dermis, the patterns of which were found to be more widely and deeply distributed compared to those in the experiment over 500 ms (Figures 3H and I). However, the PECN area could not be found in skin specimens that were subjected to the 5000-ms treatment. Compared with the corresponding experiment at frequencies of 0.5 and 1 MHz, in the 2-MHz RF treatments, the PECN area was usually smaller, degree of IENT was lower, and patterns of thermal collagen changes were more homogeneous.

### Radiofrequency Treatment-Induced Tissue Reactions with PCC

Compared to the corresponding experiments without PCC, the PCC-assisted RF treatments generated a PECN area, notably deeper within the dermis (Figure 4). RF-induced thermal tissue reactions in the upper papillary dermis were less extensive and more destructive. The zones of IENT were found in the deeper parts of the dermis, and the degree of thermal reaction was more intense in the PCC-assisted RF specimens than in each corresponding experiment without PCC. In the specimens from post-treatment days 3 and 7, histologic features of wound repair were found across all layers of the dermis, in treatments with and without PCC (Figure 5). In addition, none of the experimental settings demonstrated excessive desiccative tissue injury in the epidermis or dermis. Nonetheless, PCC-assisted RF treatments resulted in remarkably different thermal tissue reactions in the deeper dermal layers compared with RF treatments without PCC.

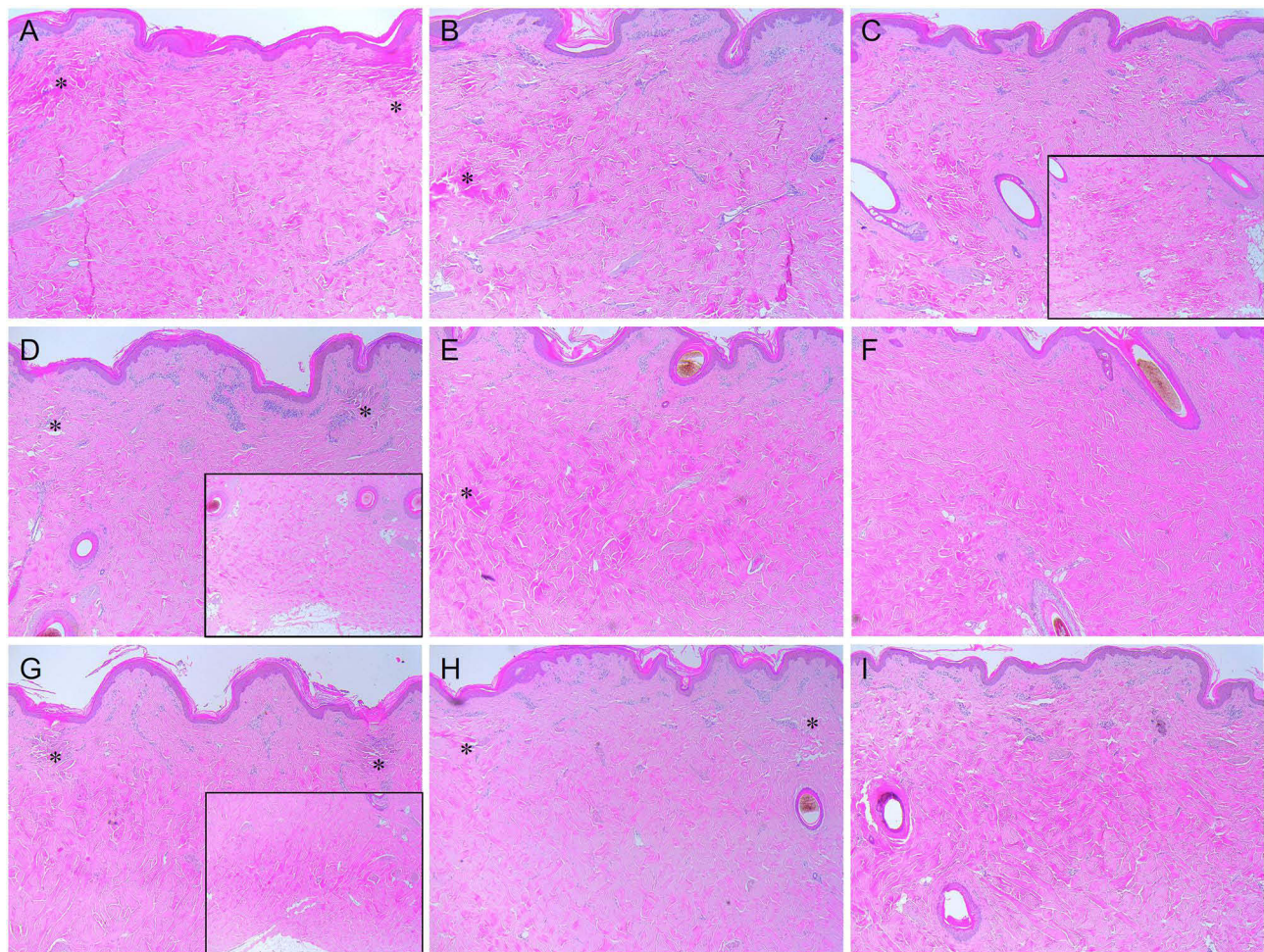


**Figure 4** Immediate tissue reactions in in vivo minipig skin after PCC-assisted RF treatment. The skin of minipig was treated with RF at the frequencies of (A-C) 0.5 MHz, (D-F) 1 MHz, and (G-I) 2 MHz and the total treatment time and number of sub-pulse packs of (A, D and G) 500 ms and single pulse pack, (B, E and H) 1000 ms and six sub-pulse packs, and (C, F and I) 5000 ms and 10 sub-pulse packs. Inset, histological photographs showing the mid and deep dermis. Asterisks, peri-electrode coagulative necrosis zones. Hematoxylin and eosin staining. Original magnification  $\times 40$ .

In the specimens from post-treatment day 14 after RF treatment without PCC, histological features of wound repair and neocollagenesis were still found, which were more distinguishable in the upper and mid-dermis than in the lower dermis (Figure 6). In particular, RF frequencies of 0.5 and 1 MHz generated more remarkable RF-induced late thermal tissue reactions in the upper dermis than those of 2 MHz. The experimental settings of PCC-assisted RF treatment exhibited distinct late thermal tissue reactions over all dermal layers (Figure 7). Compared with the corresponding experiments without PCC, PCC-assisted experiments resulted in a greater intensity of RF-induced delayed tissue reactions, which were found in the deeper layers of the dermis. Regardless of the PCC settings, when increasing the number of sub-pulse packs and decreasing the RF conduction time of each sub-pulse pack, although the total RF conduction time was identical, the patterns of neocollagenesis in RF-induced late tissue reactions during wound healing appeared to become finer and more homogeneous over more dermal layers.

## Discussion

In this study, we assessed the effects of PCC on thermal reactions caused by RF treatment using an in vivo minipig skin model. Various RF treatment conditions were used in our study; however, the equivalent amount of RF energy was given across the experimental conditions. Our data showed that regardless of PCC, RF treatments at 500 ms and a single pulse pack generated noticeable PECN and IENT in the dermis. Conversely, using 5000 ms and 10 sub-pulse packs produced distinct IENT in

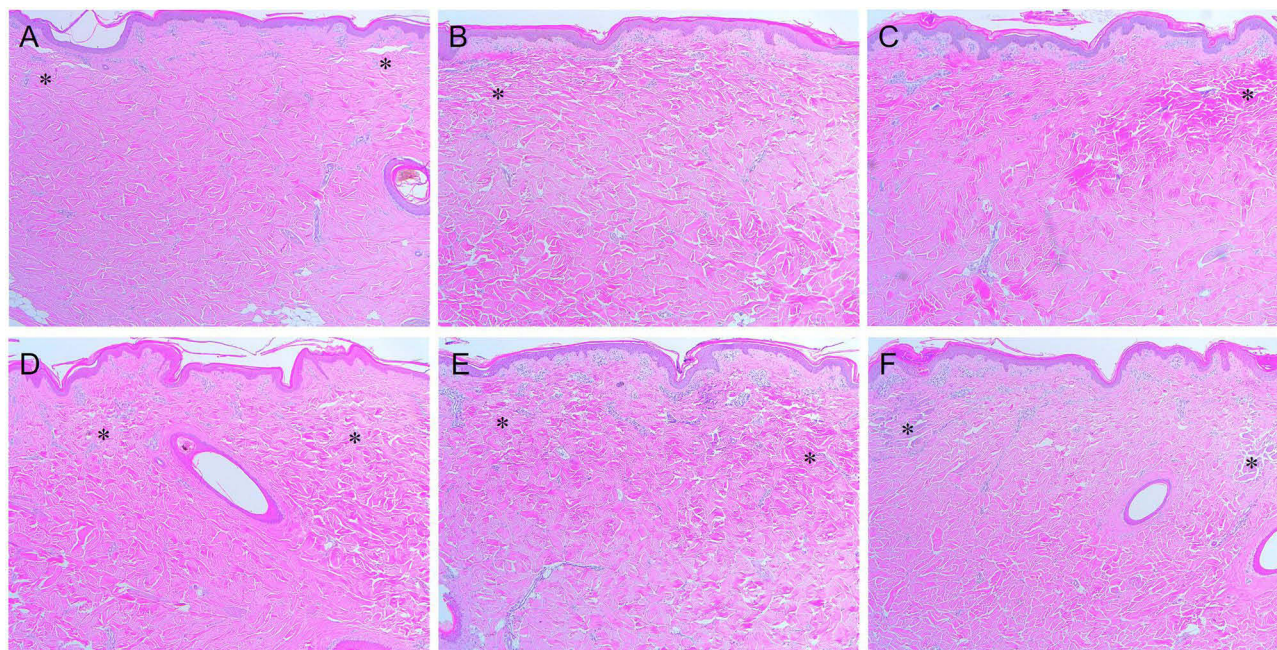


**Figure 5** Tissue reactions on day 3 in vivo minipig skin after RF treatment. RF energy was delivered to minipig skin (A-C) without PCC and (D-F) with PCC at frequencies of (A and D) 0.5, (B and E) 1 MHz, and (C and F) 2 MHz, a total treatment time of 500 ms, using a single pulse pack. Asterisks, peri-electrode coagulative necrosis zones. Hematoxylin and eosin staining. Original magnification  $\times 40$ .

a wide area of the dermis, but no PECN was found. These findings are in agreement with our previous in vivo rat skin study.<sup>5</sup> Additionally, in this study, we observed that the patterns of the PECN and IENT also varied based on the RF frequencies in otherwise identical treatment settings.

Skin cooling during dermatological treatments is clinically associated with increasing patient tolerability to painful procedures and lowering the risk of side effects by preventing thermal injury to the epidermis.<sup>9,10</sup> In this study, the PCC was achieved by employing an active cooling system using a cooled sapphire metal plate, which was integrated into the handpiece. Thermometric images taken immediately after RF energy delivery revealed two distinct temperature zones: 1) the central squared area, which corresponded to the disposable RF tip, and 2) the marginal area, which exhibited marked hypothermic features.

According to our thermometric data, immediate contact cooling effects on the surface of the PCC-assisted RF-treated skin were obtained by the direct contact cooling effects of the chilled metal plate, which significantly lowered the superficial temperature of the skin. Post-treatment removal of the cooled metal plate and RF tip from the skin resulted in the late cooling effects, merging the RF-treated central area with a hypothermic marginal area for over 60s. These reactions effectively lowered the skin's surface temperature for a particular period, thereby preventing thermal injury to the epidermis. Interestingly, the PCC also inhibited the superficial spread of RF-induced thermal reactions beyond the squared margins. Without PCC, RF-induced thermal changes increased the superficial temperature of the skin immediately after RF treatment and spread out of the squared margin over a duration of 60s. Clinically, the patient's facial or neck skin is usually treated with hundreds of shots of bipolar alternating current and microneedling RF, with or without overlap among the shots. Theoretically, heat spreading from one RF shot without a PCC through the superficial parts of the skin can affect the thermal reactions in the area adjacent to another RF shot. We suggest that the PCC can also prevent unexpected cumulative thermal damage to the upper parts of the skin, enabling practitioners to deliver multiple RF shots more safely on the patient's skin.

The effects of PCC on the RF-induced early and late histological changes were also evaluated in this study. In all experimental settings, skin specimens with PCC-assisted RF treatments demonstrated a higher degree of thermal tissue reactions in the deeper parts of the dermis compared with RF treatments without PCC. These findings suggest PCC-assisted RF treatment led to prolonged non-necrotic thermal reactions by preventing heat from spreading to the epidermis and upper papillary dermis. However, no significant desiccative tissue injury was observed in the entire dermis over 14 days in any of the experimental conditions.



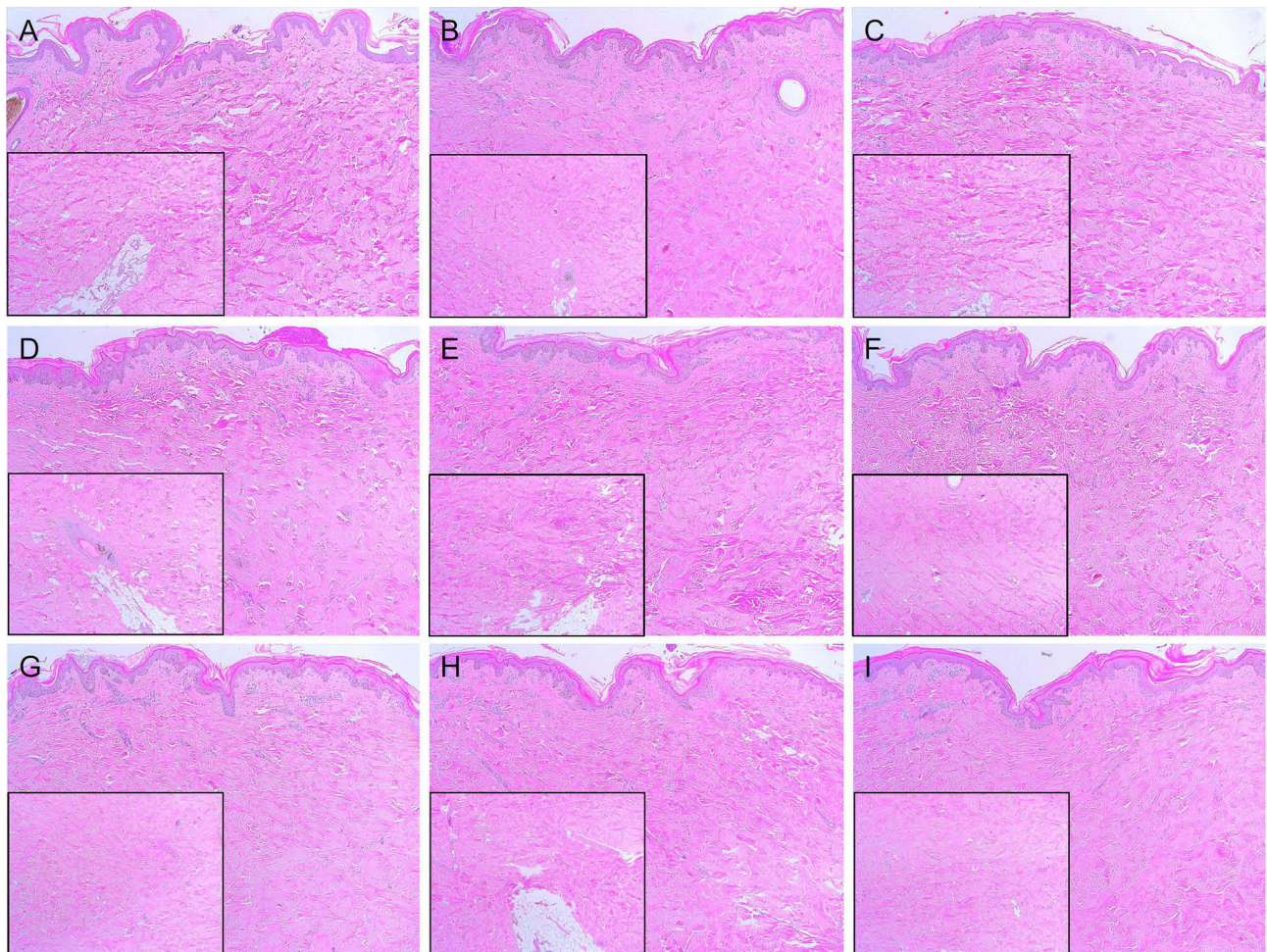


**Figure 6** Tissue reactions on day 14 in *in vivo* minipig skin after RF treatment without PCC. The skin of minipig was treated with RF at the frequencies of (A-C) 0.5 MHz, (D-F) 1 MHz, and (G-I) 2 MHz and the total treatment time and number of sub-pulse packs of (A, D and G) 500 ms and single pulse pack, (B, E and H) 1000 ms and six sub-pulse packs, and (C, F and I) 5000 ms and 10 sub-pulse packs. Inlet, histological photographs showing the mid and deep dermis. Hematoxylin and eosin staining. Original magnification  $\times 40$ .

Although PCC effectively protected the skin's superficial layers from excessive thermal injury, minipig skin specimens obtained on days three and seven exhibited noticeable histological changes in RF-induced tissue regeneration in the upper papillary dermis. These histological findings suggest that PCC-assisted RF treatment can be used for deep dermal tissue rejuvenation, as well as for treating fine wrinkles, enlarged pores, and uneven skin textures. However, PCC-assisted RF treatment on the epidermis and upper papillary dermis appeared to induce less thermal tissue reaction compared to that of RF treatments without PCC. Our histological findings of early tissue reactions to RF treatment with or without PCC indicated that early reactions were strongly correlated with late tissue reactions in minipig skin specimens collected on post-treatment day 14. Therefore, the histological features of wound repair and neocollagenesis were still observed, and the patterns and locations of collagen formation differed among experimental settings. These findings indicate that PCC could safely and effectively regulate both early and late tissue reactions across various RF parameter settings. Nevertheless, additional quantitative analyses of the effects of PCC on RF-treated skin are required to substantiate our findings.

Our study has the following limitations: 1) We utilized an observational and descriptive investigation, which limited our ability to draw causal conclusions; 2) Our thermometric and histological studies were conducted on an *in vivo* minipig skin model. Minipig skin differs from human facial and neck skin such that it contains more abundant collagen fibers and fewer skin appendages than human skin. This distinction should be considered when extrapolating our findings to human subjects; and 3) we employed a limited set of RF parameters in our study, which means that our findings may not universally apply to all treatment conditions. Importantly, our data do not indicate that using PCC during bipolar microneedling RF treatment can

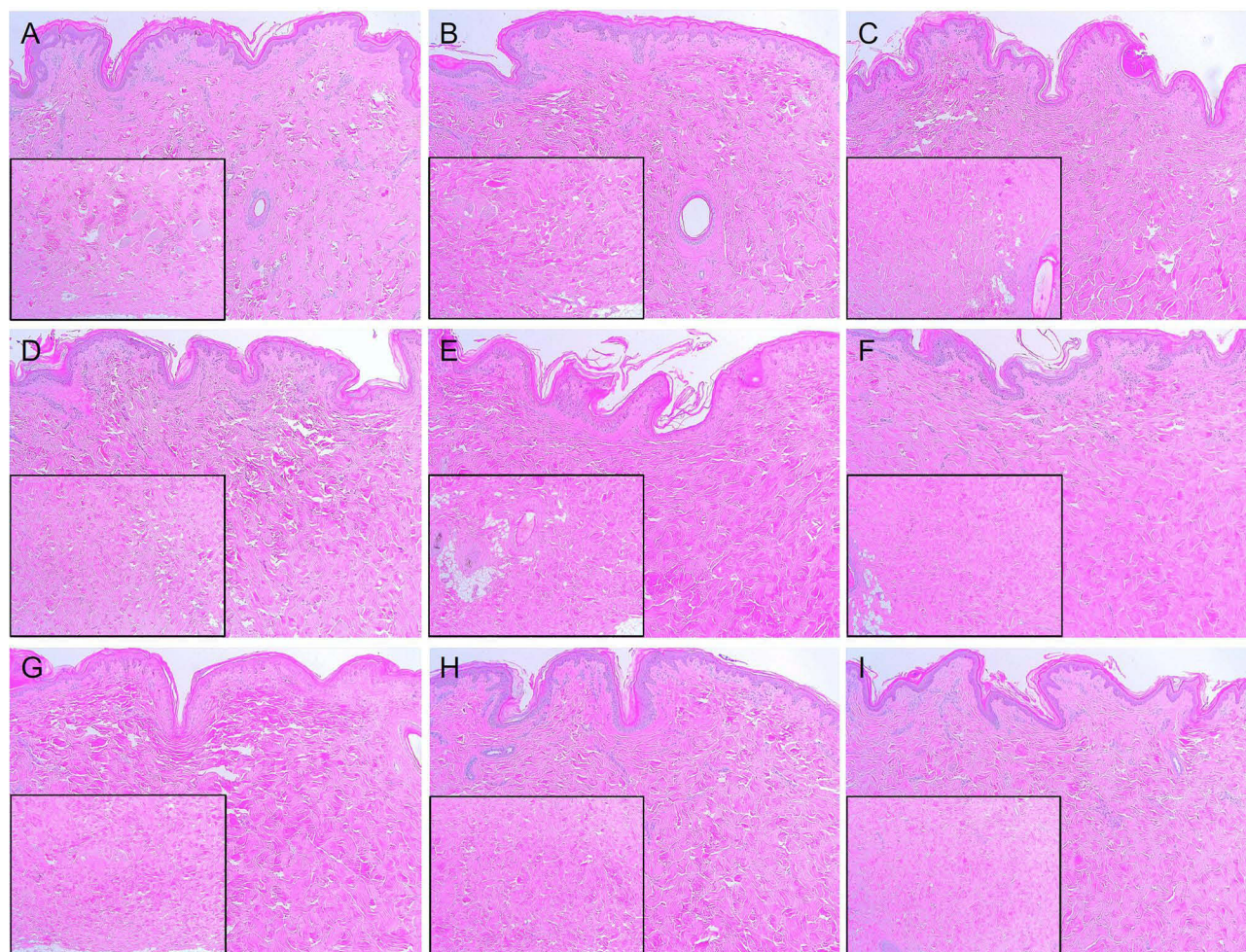


**Figure 7** Tissue reactions on day 14 in vivo minipig skin after PCC-assisted RF treatment. The skin of minipig was treated with RF at the frequencies of (A-C) 0.5 MHz, (D-F) 1 MHz, and (G-I) 2 MHz and the total treatment time and number of sub-pulse packs of (A, D and G) 500 ms and single pulse pack, (B, E and H) 1000 ms and six sub-pulse packs, and (C, F and I) 5000 ms and 10 sub-pulse packs. Inlet, histological photographs showing the mid and deep dermis. Hematoxylin and eosin staining. Original magnification  $\times 40$ .

always protect the epidermis and upper dermis from excessive thermal injury for all treatment parameters. Therefore, it is crucial to select appropriate and safe treatment parameters and protocols by taking into account patient skin characteristics and therapeutic purposes to optimize therapeutic outcomes and avoid potential adverse events.

## Conclusion

In this study, we evaluated the effect of PCC on RF-induced thermal tissue reactions in an in vivo minipig skin model after bipolar alternating-current microneedling RF treatment. The RF treatments were conducted at frequencies of 0.5, 1, and 2 MHz, with total treatment times of 500 ms for a single pulse pack, 1000 ms for six sub-pulse packs, and 5000 ms for ten sub-pulse packs. These treatments were delivered with or without PCC. Our data revealed that PCC significantly enhanced RF-induced skin reactions within the mid-to-deep dermal layers while effectively preserving the epidermis and upper papillary dermis from excessive thermal tissue injury in both the early and late stages of wound healing and tissue regeneration. However, further controlled in vivo clinical studies are necessary to validate the observed RF-induced skin under defined conditions and establish the optimal treatment parameters for medical purposes.

## Data Sharing Statement

Data supporting the findings of this study are available upon request from the corresponding authors. The data are not publicly available because of privacy and ethical restrictions.

## Statement of Ethics

All experimental protocols were approved by the Ethics Committee of the Institutional Animal Care and Use Committee of CRONEX Inc., Cheongju, Korea (CRONEX-IACUC:202210005).

## Acknowledgments

This research was supported by the Basic Science Research Program through the National Research Foundation of Korea (NRF), funded by the Ministry of Education (NRF-2020R1A6A1A03043283). We would like to thank Dongju Kim (Shenb Co., Ltd., Seoul, Korea) for his kind support in preparing the illustrations.

## Author Contributions

All authors made a significant contribution to the work reported, whether that is in the conception, study design, execution, acquisition of data, analysis, and interpretation, or in all these areas; took part in drafting, revising, or critically reviewing the article; gave final approval of the version to be published; agreed on the journal to which the article has been submitted; and agreed to be accountable for all aspects of the work.

## Funding

No funding was received for this article.

## Disclosure

The authors declare no competing financial interests. The authors declare no conflicts of interest.

## References

1. Chu KF, Dupuy DE. Thermal ablation of tumours: biological mechanisms and advances in therapy. *Nat Rev Cancer*. 2014;14(3):199–208. doi:10.1038/nrc3672
2. Golberg A, Bruinsma BG, Uygun BE, Yarmush ML. Tissue heterogeneity in structure and conductivity contribute to cell survival during irreversible electroporation ablation by electric field sinks. *Sci Rep*. 2015;5:8485. doi:10.1038/srep08485
3. Yarmush ML, Golberg A, Serša G, Kotnik T, Miklavčič D. Electroporation-based technologies for medicine: principles, applications, and challenges. *Annu Rev Biomed Eng*. 2014;16(1):295–320. doi:10.1146/annurev-bioeng-071813-104622
4. Golberg A, Yarmush ML. Nonthermal irreversible electroporation: fundamentals, applications, and challenges. *IEEE Trans Biomed Eng*. 2013;60(3):707–714. doi:10.1109/TBME.2013.2238672
5. Kim HK, Kim HJ, Kim JY, et al. Immediate and late effects of pulse widths and cycles on bipolar, gated radiofrequency-induced tissue reactions in vivo rat skin. *Clin Cosmet Invest Dermatol*. 2023;16:721–729. doi:10.2147/CCID.S404631
6. Choi M, Lee HS, Kim HJ, Kim H, Kim B, Cho SB. Effect of pulse widths and cycles on invasive, bipolar, gated radiofrequency-induced thermal reactions in ex vivo bovine liver tissue. *Clin Cosmet Invest Dermatol*. 2023;16:87–97. doi:10.2147/CCID.S395072
7. Zheng Z, Goo B, Kim DY, Kang JS, Cho SB. Histometric analysis of skin-radiofrequency interaction using a fractionated microneedle delivery system. *Dermatol Surg*. 2014;40(2):134–141. doi:10.1111/dsu.12411
8. Zhang B, Moser MAJ, Zhang EM, Luo Y, Zhang W. A new approach to feedback control of radiofrequency ablation systems for large coagulation zones. *Int J Hyperthermia*. 2017;33(4):367–377. doi:10.1080/02656736.2016.1263365
9. Wanner M, Avram M, Gagnon D, et al. Effects of non-invasive, 1210 nm laser exposure on adipose tissue: results of a human pilot study. *Lasers Surg Med*. 2009;41:401–407. doi:10.1002/lsm.20785
10. Das A, Sarda A, De A. Cooling Devices in Laser therapy. *J Cutan Aesthet Surg*. 2016;9(4):215–219. doi:10.4103/0974-2077.197028

Clinical, Cosmetic and Investigational Dermatology

Dovepress

Publish your work in this journal

Clinical, Cosmetic and Investigational Dermatology is an international, peer-reviewed, open access, online journal that focuses on the latest clinical and experimental research in all aspects of skin disease and cosmetic interventions. This journal is indexed on CAS. The manuscript management system is completely online and includes a very quick and fair peer-review system, which is all easy to use. Visit <http://www.dovepress.com/testimonials.php> to read real quotes from published authors.

Submit your manuscript here: <https://www.dovepress.com/clinical-cosmetic-and-investigational-dermatology-journal>